

Electronic Raman scattering in heavily doped *p*-type germanium

Joachim Wagner* and Manuel Cardona

Max-Planck-Institut für Festkörperforschung, Heisenbergstrasse 1, D-7000 Stuttgart 80, Federal Republic of Germany

(Received 17 June 1985)

With the use of a KCl:Tl color-center laser, light scattering by free carriers has been studied in heavily doped *p*-type germanium with the incident-photon energy resonant with the E_0 gap. The doping levels investigated range from 8.5×10^{18} up to $2 \times 10^{19} \text{ cm}^{-3}$. The electronic contribution to the Raman spectrum shows up as a broad and intense band with the maximum shifted relative to the laser frequency by approximately the Fermi energy of the holes. This electronic scattering arises predominantly from interband excitations of electrons from the light-hole into the heavy-hole valence band. The theory for the electronic scattering efficiency, which assumes wave-vector conservation, gives only an incomplete description of the observed Raman spectrum. This emphasizes the importance of transitions without wave-vector conservation for the light scattering by electronic excitations in this material. The Raman phonon shows a strong asymmetry due to a Fano interference with the electronic continuum. The line shape is found to depend strongly on the corresponding hole concentration. The absolute scattering efficiencies have been determined for both the electronic and the phonon scattering. For the phonon efficiency an order-of-magnitude decrease is observed as compared to intrinsic material.

I. INTRODUCTION

Free carriers in semiconductors introduced by heavy doping can be observed in Raman scattering.¹ Interband and intraband excitations of the free carriers can interfere with the zone-center optic phonon and produce Fano-type asymmetric line shapes.¹ For heavily doped *p*-type Si the electronic Raman scattering, as well as the effect of heavy doping on the one-phonon Raman spectrum, have been studied in detail.²⁻⁷ For *p*-type Ge, however, only the Fano-type asymmetry of the one-phonon Raman line has been investigated.^{8,9}

Electronic Raman scattering in Ge has been reported by Doehler, Colwell, and Solin using the $2.1\text{-}\mu\text{m}$ radiation of an *ABC*-YAG (yttrium-aluminum-garnet) laser.^{10,11} They studied pure and doped samples with carrier concentration in the range from 10^{15} to 10^{17} cm^{-3} . For *n*-type samples valley-orbit as well as single-particle scattering was observed,^{10,11} whereas the spectral features in the Raman spectra of *p*-type samples remain unexplained.¹⁰ More heavily doped *n*-type samples show scattering by plasmons¹² and by intervalley density fluctuations.¹³

In this study we present electronic and vibronic Raman spectra of heavily doped *p*-type germanium ($p = 10^{18} - 10^{19} \text{ cm}^{-3}$). The spectra were measured using a tunable color-center laser for the excitation with photon energies just below the E_0 gap (0.85 eV for the present carrier concentrations¹⁴). Excitation with these photon energies has the advantage of a relatively large scattering volume because only indirect valence to conduction-band absorption is possible.¹⁵ Another advantage of this laser for studying light scattering by free holes is the resonant enhancement of the scattering intensity for photon energies close to the E_0 gap.

The electronic scattering shows up as a broad band with its maximum at an energy shift roughly equal to the hole

Fermi energy. This band arises from momentum-conserving as well as nonconserving interband excitations of free holes. The scattering of light by the 304-cm^{-1} Raman phonon shows a strong interference with the electronic continuum. From the the present experiments, the absolute cross section for both the electronic and the phonon scattering are determined.

In Sec. II of this paper we give a description of the experimental setup. The experimental results are presented in Sec. III and discussed in Sec. IV. In Sec. V the conclusions are given.

II. EXPERIMENTAL DETAILS

The samples used in the present study were bulk-doped with gallium, having carrier concentrations in the range from 8.5×10^{18} to $2 \times 10^{19} \text{ cm}^{-3}$. Backscattering was observed for (111) and (110) surfaces polished with Syton. The carrier concentration was determined from the minimum in the infrared reflectivity.¹⁶ For the Raman experiments the samples were cooled down to 5 K. A KCl:Tl color-center laser^{17,18} pumped optically by the 1064-nm line of a Nd³⁺-YAG laser was used to excite the spectra. At $1.49 \mu\text{m}$ the output power of the color-center laser was typically 400 mW at an output coupler transparency of 25%. The scattered light was analyzed with a 1-m double spectrometer and detected by a cooled intrinsic Ge photodiode.

Comparing the sensitivity of the experimental setup used for the present study with the system used by Doehler *et al.*,¹⁰ an improvement by a factor of ~ 10 is found. This value is due mainly to the ~ 500 -times-higher sensitivity of the Ge diode compared to the PbS detector in the setup described in Ref. 10. This increase in sensitivity is only partially offset by the lower output power of the color-center laser ($\sim \frac{1}{20}$ th of the output of

the ABC-YAG laser used by Doehler *et al.*¹⁰). For the scattering length in Ge, a typical value of ≈ 1 mm is obtained at $1.5 \mu\text{m}$ laser wavelength¹⁵ as compared to 2.3 mm estimated for $2.1\text{-}\mu\text{m}$ excitation.¹⁰ Therefore, for electronic light scattering, the system used here is as a whole about 10 times as sensitive as the one described in Ref. 10. When dealing with scattering by phonons, also the ω^4 dependence of the scattered intensity has to be taken into account. All this enhances the sensitivity ratio by a factory of 40 for scattering by phonons, regardless of other resonance-enhancement factors involving the Raman susceptibility.

III. RESULTS

Figure 1 shows typical spectra of *p*-type Ge with carrier concentrations of 8.5×10^{18} , 1.7×10^{19} , and $2 \times 10^{19} \text{ cm}^{-3}$. The spectra were recorded in backscattering configuration and the scattered light was not analyzed for its polarization. However, the transmission of the spectrometer used was about 3 times higher for light polarized parallel to the incident laser [$x(y,y)\bar{x}$ configuration] than for perpendicular polarization [$x(y,z)\bar{x}$ configuration], so that nearly polarized spectra could be obtained. The photon energy of the exciting laser was 0.835 eV . The spectra consist of

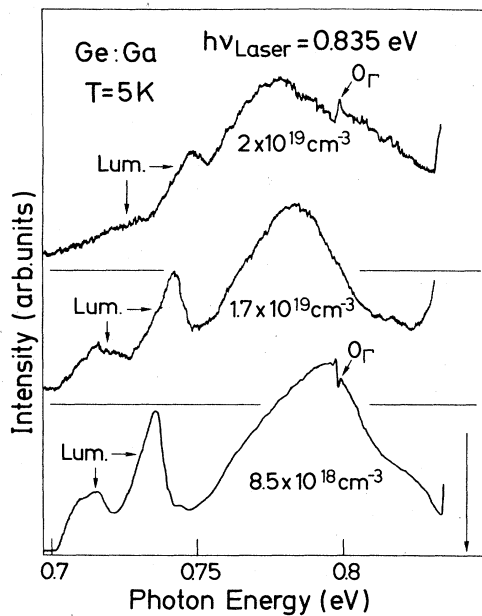


FIG. 1. Raman spectra of Ge:Ga for three different hole concentrations indicated in the figure. The spectra are not corrected for detector response. They were taken in backscattering geometry from a (111) surface ($8.5 \times 10^{18} \text{ cm}^{-3}$) or a (110) surface (1.7×10^{19} and $2 \times 10^{19} \text{ cm}^{-3}$). The incident light was polarized parallel to [110]. Because of the throughput of the monochromator the collected scattered light was mainly polarized parallel to [110]: no analyzer was used. The spectral resolution was 16 \AA (0.8 meV). O_{Γ} denotes the zone-center optical phonon and Lum. indicates indirect band-to-band luminescence. The arrow on the energy scale shows the incident-laser-photon energy.

a broad band at $\sim 0.78 \text{ eV}$ with its maximum shifting to lower photon energies with increasing hole concentration. Superimposed to this band is the Raman phonon line (O_{Γ}) at 0.798 eV , corresponding to a Raman shift of 37.7 meV (304 cm^{-1}). The two peaks at photon energies below 0.75 eV arise from the radiative recombination of photoexcited carriers across the indirect gap of germanium.¹⁴ The spectral shape of these luminescence peaks is distorted due to the cutoff in the sensitivity of the Ge detector at 0.7 eV .

The O_{Γ} phonon line, which is only observed for the two samples with the lowest and the highest carrier concentration, shows a strongly asymmetric shape, as seen in Fig. 2. Going from 8.5×10^{18} to $2 \times 10^{19} \text{ holes/cm}^3$, the asymmetry is inverted and, for the sample with the intermediate concentration of $1.7 \times 10^{19} \text{ holes/cm}^3$, no O_{Γ} phonon line is observed within the noise limit. For the samples with the lowest carrier concentration, the intensity of the scattered light was strong enough to record Raman spectra with the color-center laser tuned between 0.815 and 0.85 eV . At these two photon energies the output power of the laser dropped to about 50% of the value in the center of the tuning curve at 0.83 eV ($\sim 1.5 \mu\text{m}$).

The position of the O_{Γ} Raman line as well as the peak position of the broad band observed in the Raman spectra is plotted in Fig. 3 versus the incident-photon energy. For comparison also the position of the two luminescence peaks, which is independent of the incident-photon energy, is plotted. The broad band, however, shifts parallel to the O_{Γ} Raman line, showing that also this band arises from inelastic light scattering. Polarized Raman measurements show a partial polarization, which corresponds to a

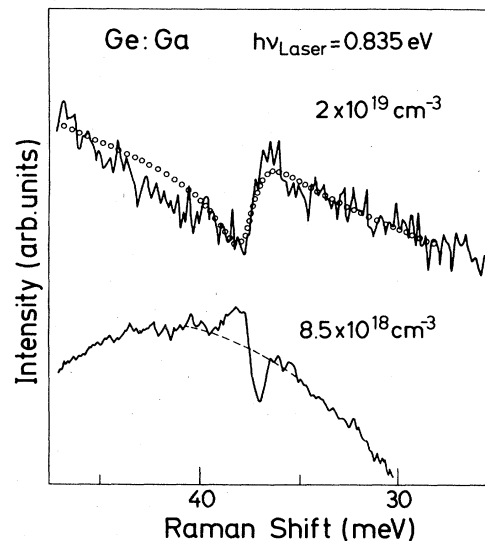


FIG. 2. Raman spectra of the zone-center optical phonon in Ge:Ga with two different hole concentrations. The zero of the vertical scale is suppressed. The spectral resolution was 16 \AA (0.8 meV). The dashed line in the lower spectrum shows the estimated background of electronic scattering, the dotted curve in the upper spectrum is a fit using Eq. (5). For details, see text.

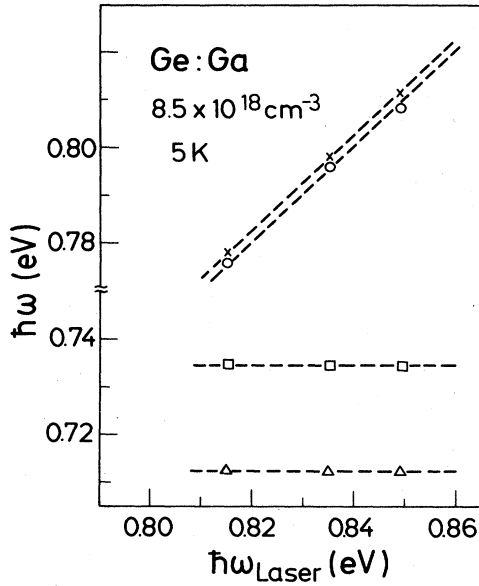


FIG 3. Shift of phonon Raman line and of the peak of the electronic spectrum versus incident-photon energy (circles and crosses). For comparison also the peak positions of the two luminescence lines observed are shown (triangles and squares).

Raman tensor with $\Gamma_{25'}$ symmetry. Changing the experimental configuration from forbidden to allowed, with respect to the $\Gamma_{25'}$ symmetry, an increase in scattered intensity by about 20% is observed. This is also consistent with the strong interference of this band with the O_{Γ} phonon, which also has $\Gamma_{25'}$ symmetry. Based on the fact that this light-scattering process is only observed in *p*-type germanium, and that the position of its maximum varies with the carrier concentration, we conclude that this band is due to electronic excitations within the valence band.

IV. DISCUSSION

A. Electronic scattering

As discussed above, we conclude from our experiments that the broad band observed in the Raman spectrum of

heavily doped *p*-type Ge for incident-photon energies nearly resonant with the E_0 gap arises from light scattering by electronic excitations. Scattering by plasmons, as observed in *n*-type Ge,¹² can be excluded as the origin of this band for the following reasons. Plasmon scattering is only observable in the Raman spectrum for incident and scattered light with the same polarization. The band under discussion, however, is also observed for crossed polarizations. Furthermore, in all the samples studied the frequency shift of the maximum of this band is smaller than the frequencies of the corresponding hole plasmons.

Single-particle intraband excitations for a *p*-doped semiconductor such as Ge can be caused either by spin-density fluctuations,¹⁹ by fluctuations of the quadrupole moment of the holes, or by mass fluctuations.^{6,20} For the two former scattering mechanisms the spectrum extends from zero Raman shift to a maximum shift $\omega_{\max} \sim qv_F$.^{19,20} The latter is expected to be small for Ge.⁶ Here, q is the wave vector transferred from the incident photon to the electronic excitation and v_F is the Fermi velocity. For backscattering geometry and an incident-photon energy of 0.83 eV, $\hbar\omega_{\max} \sim qv_F\hbar$ lies in the range of 5–10 meV for the hole concentrations studied here ($8.5 \times 10^{18} - 2 \times 10^{19} \text{ cm}^{-3}$). Thereby, only the heavy holes were taken into account, because their concentration is much larger than that of the light holes due to the large difference in effective mass.²¹ From this consideration we conclude that single-particle intraband excitations may only contribute to the observed electronic Raman spectrum for relatively small frequency shifts.

To account for the part of the spectrum for $\omega > qV_F$, inter-valence-band scattering has to be considered.^{22–24} In this scattering process, an electron is excited out of a filled state in the light-hole band into an empty state in the heavy-hole band. The corresponding scattering cross section is expected to show a strong resonance enhancement for incident-photon energies close to the E_0 gap.^{23,24} Such a resonant scattering process is shown schematically in Fig. 4.

The scattering efficiency per unit solid angle Ω and per unit frequency shift ω for such an inter-valence-band scattering can be written as²⁴

$$\left[\frac{\partial S}{\partial \Omega \partial \omega} \right]_{xx} = \left[\frac{e^2}{mc^2} \right]^2 \frac{\sqrt{2}}{45\pi^2} \omega^{1/2} \left[\frac{\omega_1 - \omega}{\omega_1} \right] \left[\frac{m^*}{\hbar} \right]^{3/2} \left[\frac{m}{m^*} \right]^2 \left[\frac{E_0}{A(\omega)} + \frac{E_0}{B(\omega)} \right]^2 \Theta(\omega - \omega_{\min}) \Theta(\omega_{\max} - \omega), \quad (1)$$

with

$$A(\omega) = E_0 + \frac{m_{hh}}{m_e} \left[\frac{m_{lh} + m_e}{m_{hh} - m_{lh}} \right] \hbar\omega - \hbar\omega_1,$$

$$B(\omega) = E_0 + \frac{m_{lh}}{m_e} \left[\frac{m_{hh} + m_e}{m_{hh} - m_{lh}} \right] \hbar\omega + \hbar\omega_1.$$

$\Theta(x)$ denotes the step function and ω_{\min} and ω_{\max} are the smallest and the largest allowed scattering frequencies,

$$\hbar\omega_{\min} = \left[1 - \frac{m_{lh}}{m_{hh}} \right] E_F, \quad (2)$$

$$\hbar\omega_{\max} = \left[\frac{m_{hh}}{m_{lh}} - 1 \right] E_F.$$

m is the free-electron mass, m_{lh} and m_{hh} are the masses of the light and heavy holes, respectively, and m_e the electron mass in the Γ conduction band. m^* is defined by

$$m^* = (m_{lh}^{-1} + m_{hh}^{-1})^{-1}. \quad (3)$$

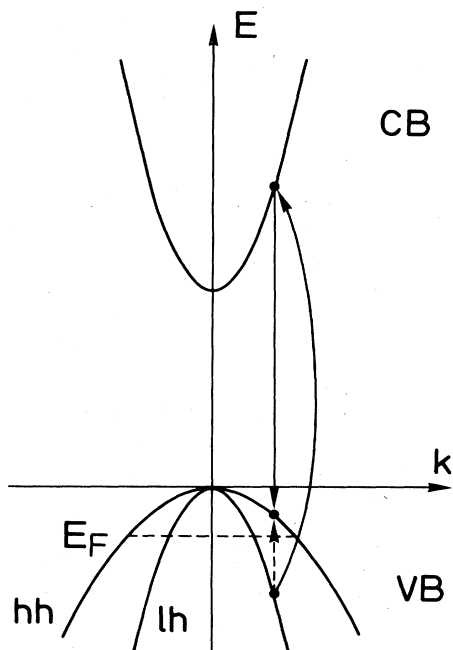


FIG. 4. Diagram of electronic inter-valence-band transitions in p -type Ge assuming wave-vector conservation.

The photon energy of the incident light is denoted by $\hbar\omega_1$. E_0 is the energy gap between the top of the valence band and the bottom of the Γ conduction band and E_F is the Fermi energy of the holes measured relative to the top of the valence band. Equation (1) is valid for incident and scattered polarization parallel to each other. Furthermore, we have used the relation $P_v^2 = m^2 E_0 / 2m^*$ instead of $P_v^2 = \frac{3}{4}(m^2 E_0 / m^*)$ given by Srivastava and Arya²² for p -type InSb. This difference arises from the much smaller spin-orbit splitting, relative to the E_0 gap energy, for Ge as compared with InSb.

The scattering efficiency $\partial S / \partial \Omega \partial \omega$ calculated from Eq. (1) is shown in Fig. 5 together with the measured spectrum. The parameters used for the calculated are $E_F = 43$ meV (8.5×10^{18} holes/cm³), $\hbar\omega_1 = 0.835$ eV, $m_{hh} = 0.347m$,²¹ $m_{lh} = 0.042m$,²¹ and $m_e = 0.038m$.²⁵ The direct-gap energy E_0 was replaced by the optical gap energy $E_{opt} = E_0 + E_F = 0.901$ eV (Ref. 14) because of the filling of the valence band. The amplitude of the calculated curve is adjusted to match the experimental intensity at the peak of the spectrum.

The calculated spectrum has its onset at $\hbar\omega_{min} = 38$ meV and it shows a pronounced enhancement for frequency shifts $\omega \sim \omega_{min}$ caused by the resonant denominator $A(\omega)$ in Eq. (1). For frequency shifts larger than ω_{min} , a fairly good agreement between the measured and the calculated spectrum is observed, whereas for $\omega < \omega_{min}$ theory cannot account for the experimentally observed scattering intensity. Intraband single-particle excitations, on the other hand, are only expected to contribute for $\hbar\omega \leq 10$ meV, as discussed above, leaving a wide gap between

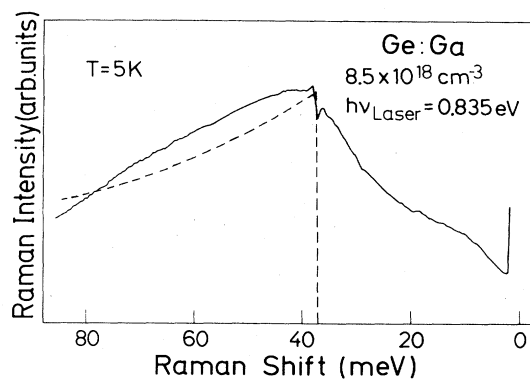


FIG. 5. Raman spectrum (drawn line) of Ge:Ga recorded in backscattering from a (111) surface with incident and scattered light polarized parallel to [110]. The spectrum has been corrected for detector response. The dashed curve is the spectrum of momentum-conserving inter-valence-band transitions calculated using Eq. (1). Parameters used for the calculation are given in the text.

$\hbar\omega > 10$ meV and $\hbar\omega < \hbar\omega_{min} = 38$ meV.

One limitation of Eq. (1) is the assumption of an isotropic valence band.²⁴ The valence bands of germanium, however, are not completely isotropic, as can be seen from the energy eigenvalues²⁶

$$E_{\pm}(\mathbf{k}) = Ak^2 \pm [B^2 k^4 + C^2(k_x^2 k_y^2 + k_y^2 k_z^2 + k_z^2 k_x^2)]^{1/2}. \quad (4)$$

The parameter C/B describes the anisotropy or warping of the bands. The positive sign refers to the light-hole and the negative sign to the heavy-hole bands. Kanehisa *et al.*²² have shown for p -type silicon that if one takes into account the anisotropy of the valence bands, interband transitions with a frequency shift smaller than ω_{min} are also allowed. Their calculated spectra of interband excitations actually resemble very much those observed here for p -type germanium. On the other hand, the valence bands of germanium are more isotropic than those of silicon, as seen from the ratio C/B , which is 1.55 for germanium and 6.47 for silicon.^{21,27} Therefore, the effect of the anisotropy on the inter-valence-band spectrum is expected to be insufficient to explain all the scattering intensity observed for $\omega < \omega_{min}$ in our p -type Ge spectra.

Another possible explanation for the low-frequency part in the experimental spectrum are inter-valence-band transitions without wave-vector conservation, contrary to the assumption of momentum conservation made in Eq. (1). Scattering processes without wave-vector conservation, as already discussed in Ref. 9 for the electronic Raman scattering in p -type germanium, also produce a spectrum with nonvanishing intensity for $\omega < \omega_{min}$. This interpretation in terms of inter-valence-band transitions without wave-vector conservation is also consistent with the incomplete vanishing of the electronic spectrum at the O_{Γ} phonon frequency. For a Fano-type line shape, a nearly vanishing scattering intensity is expected in the minimum of the asymmetric phonon Raman line (see

below). In the present spectra, however, this is not observed, indicating a considerable amount of electronic scattering incoherent with the phonon, which can be caused by additional impurity or carrier-carrier scattering, the mechanisms responsible for the wave-vector nonconservation discussed above. The Γ_1 component of the scattering with k conservation, however, should also be incoherent with the $\Gamma_{25'}$ phonon.

From the isotropic model used in Eq. (1), about 20% larger scattering intensity is expected for incident and scattered light polarized perpendicular to each other than for light with parallel polarization, irrespective of the orientation relative to the crystal axis. For a strongly anisotropic system such as holes in p -type silicon, a Raman tensor with mainly $\Gamma_{25'}$ symmetry is predicted.²⁰ The present experiments on p -type germanium show only a weak polarization (also $\Gamma_{25'}$ symmetry), which is consistent with the smaller anisotropy of the valence bands of germanium as compared with silicon.

We have also determined the absolute value of the inter-valence-band scattering efficiency at the maximum (40 meV in Fig. 5), using as reference the scattering efficiency of the O_Γ phonon in germanium.²⁸ For p -type material with 8.5×10^{18} holes/cm³, we obtain $\partial S/\partial\Omega \partial\omega = (1.7 \pm 0.9) \times 10^{-7}$ sr⁻¹/cm cm⁻¹ [backscattering from (111) plane, incident and scattered light polarized parallel to (110)], and for the sample with 2×10^{19} holes/cm, a value of $\partial S/\partial\Omega \partial\omega = (9 \pm 5) \times 10^{-8}$ sr⁻¹/cm cm⁻¹ [backscattering from (110) plane, incident and scattered light parallel to (110)] is found. From Eq. (1) we obtain theoretical values for $(\partial S/\partial\Omega \partial\omega)_{xx}$ of 5×10^{-8} and 3×10^{-8} sr⁻¹ for 8.5×10^{18} and 2×10^{19} holes/cm³, respectively. Therein, an optical gap energy of 0.901 and 0.926 eV, respectively, was used.¹⁴ The agreement between experiment and theory is satisfactory considering the limitations of the theory and the accuracy of the experimental values. The higher experimental values (as compared with theory) may be due to enhancement by the indirect transitions.

All the experimental spectra discussed so far have been

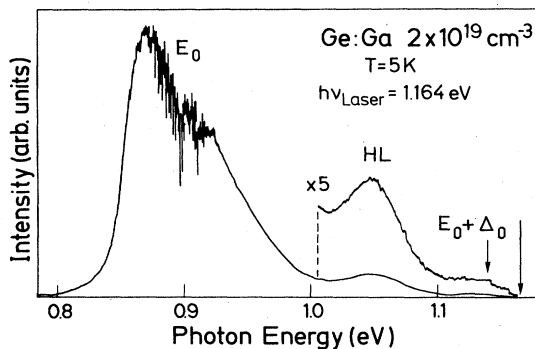


FIG. 6. Luminescence spectrum of Ge:Ga containing 2×10^{19} holes/cm³ taken with 1.164-eV exciting photon energy (indicated by an arrow on the energy scale) at a resolution of 8 Å. Emission across the E_0 and $E_0 + \Delta_0$ band gap is observed besides the hot-luminescence feature (labeled HL) discussed in the text.

taken for incident-photon energies $\hbar\omega_1$ slightly below the E_0 gap energy. Increasing $\hbar\omega_1$ to 1.164 eV, a spectrum as shown in Fig. 6 is observed. Besides the emission across the E_0 and the $E_0 + \Delta_0$ gaps, a peak (labeled HL) is found at a frequency shift ω , for which the denominator $A(\omega)$ in Eq. (1) is resonant. This peak has already been observed in Ref. 14 and corresponds to either resonance Raman scattering or hot luminescence.

B. Phonon scattering

The Raman spectra of heavily doped p -type germanium discussed here show a strong interference of the zone-center optical phonon O_Γ with the continuum of electronic inter-valence-band excitations. This discrete-continuum interaction causes a strongly asymmetric shape of the Raman phonon, which can be described by^{9,29}

$$I(\eta, \tilde{q}) = \frac{A(\tilde{q} + \eta)^2}{1 + \eta^2}, \quad (5)$$

with

$$\eta = \hbar \frac{\omega - \omega_{\text{ph}} - \Delta\omega_{\text{ph}}}{\Gamma} \quad (6)$$

and

$$\tilde{q} = \frac{VR_{\text{ph}}}{\Gamma R_e}. \quad (7)$$

A is a constant describing the intensity of the electronic scattering for frequency shifts much smaller or larger than the phonon frequency. ω_{ph} is the phonon frequency in pure material, $\Delta\omega_{\text{ph}}$ is the renormalization of ω_{ph} due to the electron-phonon interaction in the doped material, and Γ is the phonon linewidth. V is the electron-phonon matrix element and R_{ph} and R_e are the phonon Raman tensor and the Raman tensor for the electronic excitations, respectively. The strongest asymmetry is obtained for $\tilde{q} = 1$, whereas for $\tilde{q} \rightarrow \infty$ the asymmetry disappears and the line shape becomes Lorentzian. For $\tilde{q} = 0$ an inverted, symmetric notchlike antiresonance spectrum is obtained.

As can be seen from Fig. 2, the asymmetry changes from that for $\tilde{q} > 0$ ($p = 8.5 \times 10^{18}$ cm⁻³) to that for $\tilde{q} < 0$ ($p = 2 \times 10^{19}$ cm⁻³). For the sample with 2×10^{19} holes/cm³, the experimental phonon Raman line was fitted using Eq. (5). To account for the ω -dependent noninteracting electronic scattering background, a constant plus a term varying linearly in ω was added to Eq. (5). From this fit, $\tilde{q} = -0.6$ is obtained. Within the experimental resolution of 0.8 meV (6.5 cm⁻¹), no detectable shift $\Delta\omega_{\text{ph}}$ of the phonon frequency is observed. The broadening $\Gamma = 1$ meV (8 cm⁻¹) is essentially determined by the instrumental resolution. For the spectrum with $p = 8.5 \times 10^{18}$ cm⁻³, a similar analysis was not meaningful due to the strong variation of the electronic background. Olego and Cardona⁹ found, for p -type germanium with $p = 2.4 \times 10^{19}$ cm⁻³ and for incident-photon energies varying from 1.92 to 2.41 eV, $\tilde{q} \sim 25, \dots, \sim 150$, and a renormalization $\Delta\omega_{\text{ph}}$ of the phonon frequency on the order of ~ 1 cm⁻¹. Comparing their results with the present data, a consistent increase in \tilde{q} is found with increasing

incident-photon energy $\hbar\omega_1$. This can be understood in terms of the resonance of R_e for $\hbar\omega_1 \sim E_0$. Considering the small renormalization $\Delta\omega_{\text{ph}}$ reported in Ref. 9, the lack of any detectable shift in the phonon frequency in our experiment is also reasonable.

To account for the change in the sign of \tilde{q} with increasing carrier concentration, a change in sign of Raman scattering amplitude (Raman tensor) for either the phonon (R_{ph}) or the electronic scattering (R_e) has to be assumed. A change in sign of R_e , however, seems to be unlikely, because otherwise one would expect a considerable decrease in electronic scattering intensity for the sample with the intermediate concentration of 1.7×10^{19} holes/cm³, which is not observed. Assuming a change of sign for R_{ph} , an inverted, "window"-type phonon line shape is expected for $R_{\text{ph}}=0$. For $p=1.7 \times 10^{19}$ cm⁻³, however, no phonon line is observed at all within the noise limit. A possible explanation might be that the amount of electronic scattering which is coherent with the phonon scattering is too small in that particular sample to give in our experiment a detectable "window" at ω_{ph} .

In order to explain a change in sign for R_{ph} , we have to assume an additional negative contribution R_{doped} to the positive phonon Raman tensor R_{pure} of undoped material, induced by the heavy p -type doping. With the Fermi level inside the valence band, additional diagrams for phonon scattering can be constructed. A qualitative estimate shows that the interband contribution to R_{doped} has the same sign as R_{pure} , whereas the sign of the intraband contribution is the opposite of that of R_{pure} . Therefore a change in sign of R_{ph} should be possible, in principle. However, a quantitative calculation is necessary in order to decide whether the intraband contribution to R_{doped} is large enough to cause a change in the sign of R_{ph} . In addition, scattering processes without wave-vector conservation have to be taken into account, as well as direct effects of the doping on R_{pure} . Note that the resonance of the phonon Raman tensor at the E_1 gap is lowered and broadened in heavily doped germanium³⁰ and similar doping effects are expected for the resonance at the E_0 gap. Therefore no final conclusion on the cause of the reversal of the sign of \tilde{q} can be drawn.

An assumption of a change in the phonon Raman tensor with increasing doping gets further support from the

measurement of the absolute efficiency $\partial S/\partial\Omega$ of the phonon Raman scattering. From the comparison with pure germanium [$\partial S/\partial\Omega=4.5 \times 10^{-5}$ sr⁻¹ m⁻¹ for $\hbar\omega_1=0.826$ eV (Ref. 28)], we obtain $\partial S/\partial\Omega=6 \times 10^{-6}$ sr⁻¹ m⁻¹ for $p=8.5 \times 10^{18}$ cm⁻³ and $\partial S/\partial\Omega=2.4 \times 10^{-6}$ sr⁻¹ m⁻¹ for $p=2 \times 10^{19}$ cm⁻³ at $\hbar\omega=0.835$ eV. Thereby we have taken $\tilde{q}=-0.6$ for $p=2 \times 10^{19}$ cm⁻³ (as obtained from the fit) and an estimated value of $\tilde{q}=+1$ for $p=8.5 \times 10^{18}$ cm⁻³. The dropping of the scattering efficiency by more than 1 order of magnitude for $p=2 \times 10^{19}$ cm⁻³ indicates a significant effect of the p -type doping on the corresponding Raman tensor. For n -type germanium with comparable doping levels (1.9×10^{19} cm⁻³), on the other hand, the same absolute efficiency is found as for intrinsic material.³⁰

V. CONCLUSIONS

We have studied in heavily doped p -type germanium light scattering by the zone-center optical phonon and by free holes. The study was carried out for incident-photon energies close to the energy of the E_0 gap. The electronic scattering is dominated by inter-valence-band transitions. The comparison of the measured electronic Raman spectrum with the calculated spectrum of inter-valence-band excitations shows that transitions with and without wave-vector conservation contribute to the experimental spectrum. The scattering efficiency is determined from the experiments and compared with theoretical data. The phonon Raman line shows a strong Fano-type asymmetry which is attributed to the interaction of the discrete phonon line with the continuum of electronic excitations. This asymmetry is inverted when the hole concentration exceeds 10^{19} cm⁻³. A possible reason for that inversion, involving a carrier-density-dependent change of the phonon Raman tensor, is discussed. The scattering efficiency of the phonon is found to be about 1 order or magnitude smaller for heavily doped p -type material than for pure material.

ACKNOWLEDGMENTS

We would like to thank H. Hirt, M. Siemers, and P. Wurster for expert experimental assistance and to R. Sauer for a critical reading of the manuscript.

*Present address: Fraunhofer-Institut für Angewandte Festkörperphysik, Eckerstrasse 4, D-7800 Freiburg, Federal Republic of Germany.

¹See G. Abstreiter, M. Cardona, and A. Pinczuk, in *Light Scattering in Solids IV*, edited by M. Cardona and G. Güntherodt (Springer, Heidelberg, 1984).

²F. Cerdeira and M. Cardona, *Phys. Rev.* **5**, 1440 (1972).

³F. Cerdeira, T. A. Fjeldy, and M. Cardona, *Phys. Rev. B* **8**, 4734 (1973).

⁴K. Jain, Shui Lai, and M. V. Klein, *Phys. Rev. B* **13**, 5448 (1976).

⁵M. Chandrasekhar, M. Cardona, and E. O. Kane, *Phys. Rev. B* **16**, 3579 (1977).

⁶M. Chandrasekhar, U. Rössler, and M. Cardona, in *Physics of Semiconductors, 1978*, edited by B. L. H. Wilson (Institute of

Physics, Bristol, 1979), p. 961.

⁷M. Chandrasekhar, U. Rössler, and M. Cardona, *Phys. Rev. B* **22**, 761 (1980).

⁸D. Olego, H. Chandrasekhar, and M. Cardona, in *Physics of Semiconductors, 1978*, Ref. 6, p. 1313.

⁹D. Olego and M. Cardona, *Phys. Rev. B* **23**, 6592 (1981).

¹⁰J. Doehler, P. J. Colwell, and S. A. Solin, *Phys. Rev. B* **9**, 636 (1974).

¹¹J. Doehler, P. J. Colwell, and S. A. Solin, *Phys. Rev. Lett.* **34**, 584 (1975).

¹²F. Cerdeira, N. Mestres, and M. Cardona, *Phys. Rev. B* **29**, 3737 (1984).

¹³G. Contreras, A. K. Sood, and M. Cardona, *Phys. Rev. B* **32**, 930 (1985).

¹⁴J. Wagner and L. Viña, *Phys. Rev. B* **30**, 7030 (1984).

- ¹⁵W. C. Dash and R. Newman, *Phys. Rev.* **99**, 1151 (1955).
- ¹⁶V. I. Fistful, *Heavily Doped Semiconductors* (Plenum, New York, 1969), p. 234.
- ¹⁷W. Gellermann, F. Lüty, and C. R. Pollak, *Opt. Commun.* **39**, 391 (1981).
- ¹⁸L. F. Mollenauer, N. D. Vieira, and L. Szeto, *Opt. Lett.* **7**, 414 (1982).
- ¹⁹Ref. 1, p. 44.
- ²⁰V. A. Voitenko, I. P. Ipatova, and A. V. Subashiev, *Pis'ma Zh. Eksp. Teor. Fiz.* **37**, 334 (1983) [*JETP Lett.* **37**, 396 (1983)].
- ²¹*Landolt-Börnstein Tables*, edited by O. Madelung, M. Schulz, and H. Weiss (Springer, Berlin, 1982), Vol. 17.
- ²²M. A. Kanehisa, R. F. Wallis, and M. Balkanski, *Phys. Rev. B* **25**, 7619 (1982).
- ²³D. L. Mills, R. F. Wallis, and E. Burstein, in *Light Scattering in Solids*, edited by M. Balkanski (Flammarion, Paris, 1971), p. 107.
- ²⁴S. Srivastava and K. Arya, *Phys. Rev. B* **8**, 667 (1973).
- ²⁵R. L. Aggarwal, *Phys. Rev. B* **2**, 446 (1970).
- ²⁶G. Dresselhaus, A. F. Kip, and C. Kittel, *Phys. Rev.* **98**, 368 (1955).
- ²⁷J. C. Hensel and K. Suzuki, in *Proceedings of the 10th International Conference on the Physics of Semiconductors, Cambridge, Mass., 1970*, edited by S. P. Keller, J. C. Hensel, and F. Stern, CONF-700 SO1 (U.S. AEC Division of Technical Information, Springfield, Va., 1970), p. 541.
- ²⁸J. Wagner and M. Cardona, *Solid State Commun.* **53**, 845 (1985).
- ²⁹M. Chandrasekhar, M. Renucci, and M. Cardona, *Phys. Rev. B* **17**, 1623 (1978).
- ³⁰A. K. Sood, G. Contreras, and M. Cardona, *Phys. Rev. B* **31**, 3760 (1985).